

LEARNED DIGITAL CODES FOR OVER-THE-AIR FEDERATED LEARNING

A. Tarizzo, M. Kazemi, D. Gündüz

Department of Electrical & Electronic Engineering, Imperial College London, London, UK

ABSTRACT

Federated edge learning (FEEL) enables distributed model training across wireless devices without centralising raw data, but deployment is constrained by the wireless uplink. A promising direction is over-the-air (OTA) aggregation, which merges communication with computation. Existing digital OTA methods can achieve either strong convergence or robustness to noise, but struggle to achieve both simultaneously, limiting performance in low signal-to-noise ratios (SNRs) where many IoT devices operate. This work proposes a learnt digital OTA framework that extends reliable operation into low-SNR conditions while maintaining the same uplink overhead as state-of-the-art. The proposed method combines an unrolled decoder with a jointly learnt unsourced random access codebook. Results show an extension of reliable operation by more than 7 dB, with improved global model convergence across all SNR levels, highlighting the potential of learning-based design for FEEL.

Index Terms— federated edge learning, digital over-the-air computation, unsourced random access, distributed optimization, compressed sensing.

1. INTRODUCTION

Federated learning (FL) has become a well-established approach in machine learning (ML), where by keeping data local, it addresses privacy concerns and reduces reliance on centralised storage [1][2]. Naturally, this interest has extended to wireless edge devices such as phones, Internet of things (IoT) sensors, autonomous vehicles, and other low-power systems, as these devices generate large amounts of valuable and often under-utilised data [3]. However, scaling FL to the wireless edge remains challenging [4]. Each device must repeatedly upload large updates, creating a severe bottleneck at the wireless uplink. To address this, compression methods such as sparsification [5, 6], and quantisation [7][8][9] focus on reducing update size, but there is also opportunity to optimise the wireless communication method itself, merging communication and computation.

Over-the-air (OTA) aggregation tackles this by enabling devices to transmit simultaneously, exploiting the channel's linear superposition to combine updates directly [10, 11]. This avoids scheduling overheads and reduces uplink latency. Analog OTA methods transmit raw updates, but are impractical due to sensitivity to noise, fading, and precise power control [3][12]. Digital OTA instead encodes updates, providing robustness while allowing concurrent transmission [13]. However, existing designs such as massive digital over-the-air computation (MD-AirComp) fail to converge in low signal-to-noise ratio (SNR) regimes common in IoT [14]. This motivates the need for a more robust digital OTA framework where integrating learning-based techniques offers a way to improve recovery and convergence without increasing uplink overhead.

M. Kazemi's work was funded by UK Research and Innovation (UKRI) under the UK government's Horizon Europe funding guarantee [grant number 101103430].

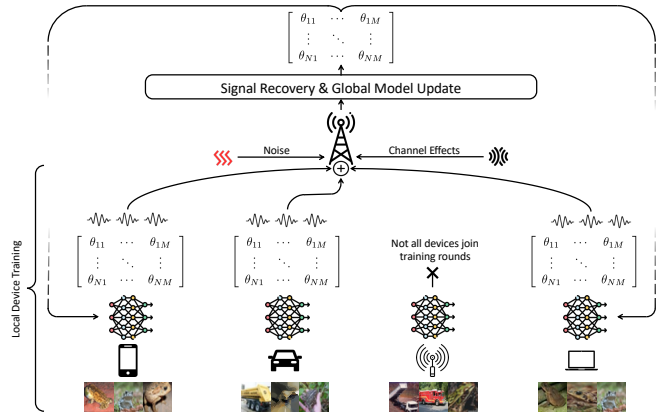


Fig. 1. Illustrative digital OTA pipeline for FEEL.

Related Works: Early implementations of FEEL used existing orthogonal multiple-access designs such as TDMA and OFDMA, where devices are allocated distinct channel resources. While simple and reliable, these approaches incur high latency since updates must be decoded individually before aggregation, making them inefficient even with modest numbers of devices. OFDMA-F²L partially addresses this by jointly optimising client selection, sub-channel allocation, and modulation, but is still constrained by the need for per-device decoding and scheduling overheads [15].

One-bit digital OTA aggregation (OBDA) takes advantage of channel's linear superposition, enabling devices to transmit simultaneously with updates combining directly in the air [13], showing that extreme quantisation could still support convergence, but with limited accuracy due to severe information loss. Frequency-shift keying with majority vote (FSK-MV) improved robustness to hardware imperfections, yet remained effectively one-bit per update and suffered the same accuracy ceiling [16]. MD-AirComp introduced a digital OTA framework combining unsourced random access (URA) [17], compressed sensing (CS), and vector quantisation (VQ) [14], which resulted in higher accuracy than analog OTA and greater efficiency than orthogonal access, but sharply degraded performance in low-SNR regimes, where symbol recovery and active-device estimation become unreliable, preventing convergence.

Proposed Solution: To the best of our knowledge, no prior work has applied learning directly within the digital OTA pipeline. The only related example is a very different approach where a neural network was used at the BS to guide power control and client scheduling, but did not address the OTA transmission and decoding process itself [18]. As such, learning-based optimisation of both the encoder and decoder for digital OTA aggregation remains unexplored, motivating this work. The contributions of this paper are threefold:

- **Improved Performance:** This work proposes a new solution for digital OTA FEEL that extends reliable operation into low-SNR environments. Building on the MD-AirComp framework, the approach

extends feasible operation by more than 7 dB of noise, while also improving reliability across the full SNR range. Crucially, this has been achieved with no additional uplink overhead or reduction in channel-efficiency.

- **Strong Generalisation:** The approach generalises effectively to unseen setups, including different global models, highly non-IID device distributions, and varying numbers of active devices, in both high- and low-SNR regimes.

- **Broader Implications:** Jointly learning the URA codebook was shown to systematically outperform fixed constructions, with implications for any method relying on URA representations. Local training at the BS, even on very small non-IID subsets, was also shown to capture representative device-level training dynamics.

Notation: lower-case, bold lower-case, and bold upper-case denote scalars, vectors, and matrices, respectively. \mathbf{I}_d denotes the $d \times d$ identity matrix. x_i indicates the i -th entry of x , X_i the i -th column of \mathbf{X} , and X_{ij} the element in the i -th and j -th column j of \mathbf{X} . p -norms is denoted by $\|\cdot\|_p$. \odot and *circ* denote element-wise multiplication and exponentiation, respectively. Superscripts in parentheses indicate the number of iteration or layer. Expectation, variance, and covariance are denoted by $\mathbb{E}[\cdot]$, $\text{Var}(\cdot)$, and $\text{Cov}(\cdot, \cdot)$, respectively.

2. SYSTEM MODEL

We consider FEEL among K_t edge devices, of which a random subset of K_a devices are active per round. Each device k has a single antenna and local dataset \mathcal{D}_k . For simplicity, datasets are assumed equal size $|\mathcal{D}_k| = B$ and devices have equal compute capability. In practice, heterogeneity in data and hardware affects participation dynamics, but this is abstracted away [19]. The base station (BS) is modelled as a single-antenna receiver co-located with the parameter server, responsible for decoding, aggregation, and broadcasting the updated global model. Synchronisation is assumed so that simultaneous transmissions align in time and frequency [20]. The distributed learning task is to minimise the average empirical loss:

$$\min_{\mathbf{w} \in \mathbb{R}^W} f(\mathbf{w}) = \frac{1}{K_t} \sum_{k=1}^{K_t} F_k(\mathbf{w}), \quad (1)$$

where $\mathbf{w} \in \mathbb{R}^W$ is the global model parameter vector and $F_k(\mathbf{w})$ is its empirical loss on dataset \mathcal{D}_k . At the start of round t , the BS broadcasts the updated global model parameters at round $t-1$, \mathbf{w}^{t-1} , to all devices. Each active device then performs E local stochastic gradient descent (SGD) steps to produce \mathbf{w}_k^t , making the update

$$\Delta \mathbf{w}_k^t = \mathbf{w}_k^t - \mathbf{w}^{t-1}. \quad (2)$$

To reduce uplink cost, devices transmit compressed updates. Each device maintains an error accumulator \mathbf{e}_k^t , which is added to future updates, and is updated as

$$\mathbf{s}_k^t = \Delta \mathbf{w}_k^t + \mathbf{e}_k^{t-1}, \quad \mathbf{e}_k^t = \mathbf{s}_k^t - \mathcal{Q}(\mathbf{s}_k^t), \quad (3)$$

where $\mathcal{Q}(\mathbf{s}_k^t)$ is the transmitted message, with $\mathcal{Q}(\cdot)$ denoting the compression operator. The active set in round t is \mathcal{S}_a , with $|\mathcal{S}_a| = K_a$. The BS aggregates compressed updates as

$$\mathbf{s}^t = \frac{1}{K_a} \sum_{k \in \mathcal{S}_a} \mathcal{Q}(\mathbf{s}_k^t), \quad (4)$$

and updates the global model, with the global learning rate η , as

$$\mathbf{w}^t = \mathbf{w}^{t-1} + \eta \mathbf{s}^t. \quad (5)$$

Sparse Recovery Formulation: In the uplink, each device divides its message into fixed fragments, which are then mapped to a length- d codeword from a shared URA codebook $\mathbf{C} \in \mathbb{R}^{n \times d}$, and all active devices transmit their chosen codewords simultaneously. This can be viewed as a sparse recovery problem. Let $\mathbf{x} \in \mathbb{R}^n$ denote the per-codeword activity vector, a sparse, non-negative, and integer-valued vector whose i -th element indicates how many devices chose the i -th codeword; i.e., $\|\mathbf{x}\|_0 \ll n$ and $\sum_i x_i = K_a$. The received signal is

$$\mathbf{y} = \mathbf{C}^\top \mathbf{x} + \mathbf{w}, \quad (6)$$

where $\mathbf{w} \sim \mathcal{N}(0, \sigma^2 \mathbf{I}_d)$ models the noisy channel. The BS must recover \mathbf{x} (or $\mathbf{C}^\top \mathbf{x}$) from these noisy linear measurements, which matches the canonical compressed sensing task but with additional structural constraints. This framework enables multiple devices to transmit concurrently without preambles or explicit separation, while still enabling reliable aggregate recovery in noisy conditions.

3. PROPOSED SOLUTION

To integrate a learnt scheme into FEEL, in the proposed solution, the encoder and decoder are jointly trained offline on a representative dataset, then fixed for deployment (see Section 3.2). The resulting URA codebook and decoder can be reused across tasks and communication rounds without retraining, much like a conventional un-learnt design. During each round, devices perform local training and split their update \mathbf{s}_k^t into fixed-length fragments \mathbf{u}_i . After error feedback is applied, each fragment is quantised using the current quantization codebook $\mathbf{Q} \in \mathbb{R}^{n \times d}$ broadcasted by the BS at each round. VQ is performed via a nearest-neighbour search that minimises Euclidean distance,

$$\hat{\mathbf{q}} = \arg \min_{\mathbf{q} \in \mathcal{Q}} \|\mathbf{u}_i - \mathbf{q}\|_2, \quad (7)$$

The index of each device (corresponding to $\hat{\mathbf{q}}$) is mapped to a codeword from the shared URA codebook $\mathbf{C} \in \mathbb{R}^{n \times d}$, and transmitted simultaneously with the selected codewords of other users. The BS receives the noisy linear superposition of transmitted codewords (Eq. 6) and decodes the estimated activity vector $\hat{\mathbf{x}}$. Once recovered, the BS de-quantises the corresponding entries of \mathbf{Q} , reconstructs the transmitted fragments, and aggregates them as in Eq. 4. The resulting global update is applied to the model, then broadcast back to devices together with the next-round's quantisation codebook.

3.1. Quantisation Codebook Construction

At the start of each round, the BS trains locally on its own dataset, and fragments its update into vectors of length d . These fragments are clustered with k-means++ [21], and the n resulting centroids form the quantisation codebook $\mathbf{Q} \in \mathbb{R}^{n \times d}$. The BS then quantises its fragments against \mathbf{Q} and records centroid frequencies, producing a normalised popularity distribution:

$$\hat{\pi}_i = \frac{N_i}{\sum_j N_j}, \quad (8)$$

where N_i is the number of fragments assigned to codeword i . The codebook is then ordered from most to least popular before being broadcast. The motivation for this step is that the BS's popularity distribution provides a reliable estimate of other devices' codeword usage. By applying the same ordering across all devices, the expected distribution of codeword usage is standardised across rounds and learning tasks, presenting a more consistent input distribution to the URA codebook during training, influencing its learnt structure. In addition, the decoder is able to learn that earlier codewords are more popular and use this as prior knowledge during recovery.

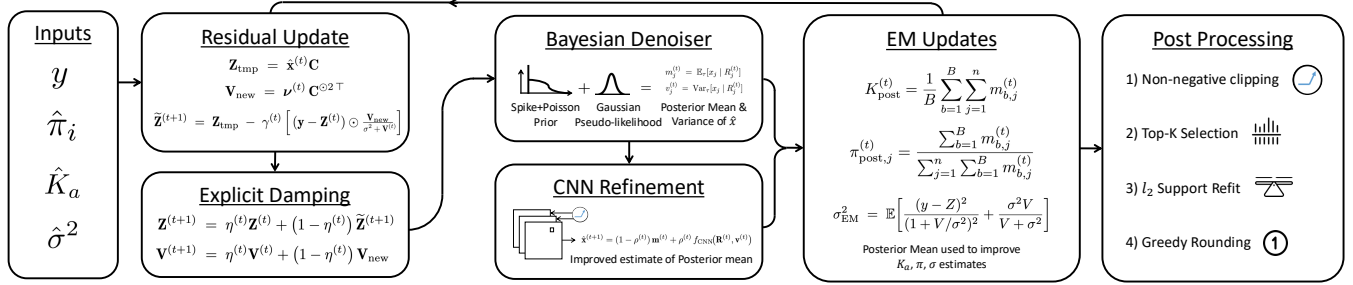


Fig. 2. AMP-DA-Net decoder structure.

3.2. AMP-DA-Net (Learned Decoder)

The core component of the proposed solution is a learned unrolled decoder, AMP-DA-Net, which builds upon approximate message passing (AMP), generalised AMP (GAMP), AMP-Net, and the AMP-based digital aggregation (AMP-DA) decoder used in MD-AirComp [22][23][14]. AMP frames decoding as a sequence of denoising tasks achieved by alternating residual updates with sparsity-promoting shrinkage and an Onsager correction term so that each residual behaves like fresh Gaussian noise. GAMP generalises this to arbitrary likelihoods and priors, splitting each iteration into an *output update* and an *input update*. AMP-Net then unrolls this iterative scheme into a fixed-depth network, replacing the shrinkage function with a CNN-based denoiser (e.g. convolution + ReLU), and learns per-layer calibration parameters such as step sizes, scaling, and damping factors. Next, we explain the working blocks of the proposed learned decoder, AMP-DA-Net, as depicted in Fig. 2.

Initialisation: Each round is initialised as

$$\mathbf{x}^{(0)} = \mathbf{0} \in \mathbb{R}^n, \quad \boldsymbol{\nu}^{(0)} = \mathbf{1} \in \mathbb{R}^n, \quad (9)$$

$$\mathbf{Z}^{(0)} = \mathbf{y} \in \mathbb{R}^d, \quad \mathbf{V}^{(0)} = \mathbf{1} \in \mathbb{R}^d, \quad (10)$$

where $\hat{\mathbf{x}}$ is the current count estimate, $\boldsymbol{\nu}$ its variance proxy in the codeword domain, \mathbf{Z} the residual in the measurement domain, and \mathbf{V} its corresponding variance proxy.

Output Block: It updates the measurement-domain residual and variance. From $\hat{\mathbf{x}}^{(t)}$ and $\boldsymbol{\nu}^{(t)}$, we compute

$$\mathbf{Z}_{\text{tmp}} = \hat{\mathbf{x}}^{(t)} \mathbf{C}, \quad \mathbf{V}_{\text{new}} = \boldsymbol{\nu}^{(t)} \mathbf{C}^{\odot 2 \top}. \quad (11)$$

where $\mathbf{x}^{\odot 2}$ denotes the element-wise square. Similar to AMP-Net, the Onsager term and matched-filter gain are absorbed into a learnable scalar $\gamma^{(t)}$, but an explicit learnable damping factor $0 < \eta^{(t)} < 1$ is added to stabilise updates:

$$\tilde{\mathbf{Z}}^{(t+1)} = \mathbf{Z}_{\text{tmp}} - \gamma^{(t)} \left[(\mathbf{y} - \mathbf{Z}^{(t)}) \odot \frac{\mathbf{V}_{\text{new}}}{\sigma^2 + \mathbf{V}^{(t)}} \right], \quad (12)$$

$$\mathbf{Z}^{(t+1)} = \eta^{(t)} \mathbf{Z}^{(t)} + (1 - \eta^{(t)}) \tilde{\mathbf{Z}}^{(t+1)}, \quad (13)$$

$$\mathbf{V}^{(t+1)} = \eta^{(t)} \mathbf{V}^{(t)} + (1 - \eta^{(t)}) \mathbf{V}_{\text{new}}. \quad (14)$$

To constrain learning, $\gamma^{(t)}$ is parametrised by a centred tanh mapping, restricted to $[0.3, 2]^1$.

Input Block: It de-noises in the codeword domain. After the measurement-domain update, each element of \mathbf{x} is treated as passing through a scalar pseudo-channel defined as,

$$\mathbf{R}^{(t)} = \hat{\mathbf{x}}^{(t)} + \frac{\text{var}_2}{\text{var}_1}, \quad (15)$$

¹Allowing values slightly above 1 introduces controlled instability, shown to improve expressiveness and convergence [24].

where $\text{var}_1 = \gamma_{\text{inv}}^{(t)} \mathbf{C}^{\odot 2}$, $\text{var}_2 = ((\mathbf{y} - \mathbf{Z}^{(t)}) \odot \gamma_{\text{inv}}^{(t)}) \mathbf{C}^{\top}$, and $\gamma_{\text{inv}}^{(t)} = \frac{\alpha^{(t)}}{\sigma^2 + \mathbf{V}^{(t)}}$. Here $R_j^{(t)}$ is the pseudo-observation for codeword j , while $\text{var}_1^{(t)}$ captures its precision. Intuitively, if the residual looks reliable (low noise, low variance), $\gamma_{\text{inv}}^{(t)}$ strengthens the correction, and vice-versa. Each element x_j is then de-noised under a spike-and-slab prior, where the spike is a point mass at zero and the slab is a Poisson distribution,

$$p(x_j) = (1 - \alpha_j) \delta_0 + \alpha_j \text{Pois}(\lambda_j), \quad (16)$$

where $\lambda_j = K_a \hat{\pi}_j$ and $\alpha_j = 1 - e^{-\lambda_j}$. This reflects that most codewords are unused (spike at zero), while active ones follow a Poisson distribution with mean λ_j . Combining this prior with the Gaussian pseudo-likelihood yields a posterior mean and variance:

$$m_j^{(t)} = \mathbb{E}_\tau[x_j | R_j^{(t)}], \quad v_j^{(t)} = \text{Var}_\tau[x_j | R_j^{(t)}], \quad (17)$$

with a per-layer temperature $\tau^{(t)}$ controlling sharpness (low τ is MAP-like, high τ improves stability at low SNR). Uncertainty follows the Bayesian update, $\boldsymbol{\nu}^{(t+1)} = \mathbf{v}^{(t)}$. Finally, we form a compact 6-channel codeword-domain feature map,

$$\boldsymbol{\Phi}^{(t)} = [\mathbf{R}^{(t)}, \sqrt{\mathbf{V}_i^{(t)}}, \mathbf{m}^{(t)}, \sqrt{\mathbf{v}^{(t)}}, \boldsymbol{\alpha}^{(t)}, \boldsymbol{\lambda}^{(t)}], \quad (18)$$

and obtain a refined estimate via the 1D CNN, that is then blended with the Bayesian mean (with $0 \leq \rho^{(t)} \leq 1$):

$$\tilde{\mathbf{x}}^{(t)} = f_{\text{CNN}}^{(t)}(\boldsymbol{\Phi}^{(t)}). \quad (19)$$

$$\mathbf{x}^{(t+1)} = (1 - \rho^{(t)}) \mathbf{m}^{(t)} + \rho^{(t)} \tilde{\mathbf{x}}^{(t)}. \quad (20)$$

EM Updates: To adapt across different setups, key statistics are refined at each layer via expectation–maximisation (EM). The posterior means $\mathbf{m}^{(t)}$ are summed to update the active-device estimate \hat{K}_a , and normalised to refresh the popularity distribution π , both smoothed with learnt step sizes via convex combinations. The noise variance σ^2 is updated by moment-matching residual energy in the log domain for stability [14]. These adaptive refinements are key to allowing the decoder to generalise across tasks and rounds.

Post-processing: Final corrections are applied to enforce task-specific structure. These include non-negativity, a top- K support projection with ℓ_2 refit on the active set, and a final greedy rounding approach. The resulting estimate $\hat{\mathbf{x}}$ is then de-quantised to reconstruct transmitted fragments, which are aggregated and normalised by \hat{K}_a to update the global model.

Dataset Collection: A perfect aggregation (PA) FEEL pipeline with error feedback, popularity ordering, and varying K_a was run to generate training data. Device codeword indices were gathered into target get sparse vectors \mathbf{x} . A ResNet [25] with highly non-IID splits was

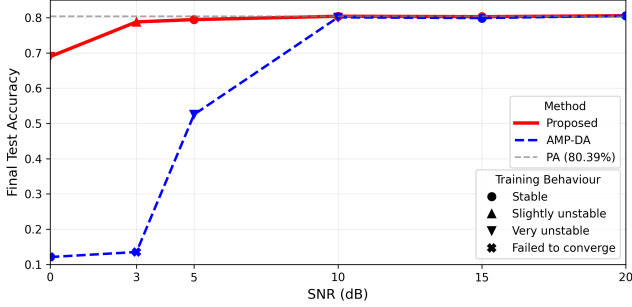


Fig. 3. Final test accuracies and training stability.

used, producing a dataset that captured key FEEL trends such as non-uniform codeword usage and per-round statistics.

Codebook Representation: The URA codebook at the encoder is jointly trained with the decoder using a two-matrix parametrisation $\mathbf{C}_{\text{syn}} = \mathbf{D}\mathbf{W}$, where $\mathbf{D} \in \mathbb{R}^{n \times d}$ stores base codeword vectors and $\mathbf{W} \in \mathbb{R}^{d \times d}$ is a learnt shear/rotation. Following the *simple VQ* (SimVQ) algorithm, this improves gradient flow, avoids *dead codewords* (rarely used ones), and stabilises training compared to learning \mathbf{C} directly [26]. Rows of \mathbf{C}_{syn} are renormalised to unit ℓ_2 norm after each update to maintain equal codeword power. For \mathbf{D} , Gaussian, Bernoulli, and a data-driven pseudo-inverse initialisation (as in iterative shrinkage/thresholding algorithm (ISTA) network (ISTA-Net) [27]) were tested, with the latter proving most effective, while \mathbf{W} was initialised as identity. This parametrisation provided smoother training and slightly higher recovery accuracy.

Loss Function: The training objective combines four terms: a mean squared error (MSE) for reconstruction $\|\hat{\mathbf{x}}_i - \mathbf{x}_i\|_2^2$, a sparsity promoting ℓ_1 penalty $\|\hat{\mathbf{x}}_i\|_1$, a regulariser for the rotation/shear matrix \mathbf{W} to remain well-conditioned $\|\mathbf{W}^\top \mathbf{W} - \mathbf{I}\|_F^2$ (following SimVQ), and a final MSE for active-device estimation with $(\hat{K}_{a,i} - K_{a,i})^2$, with hyper-parameters $\lambda_1, \lambda_W, \lambda_K$ balancing their contributions.

Hyper-parameters: Pre-training used 256,000 samples for training, 64,000 for validation, and 20,000 from held-out rounds for testing. Batch size was 64, with a maximum of 500 epochs and early stopping (patience 20, tolerance 10^{-6}). Optimisation used Adam with learning rate 10^{-4} , which halved if validation loss did not improve for 10 epochs. Gradients were accumulated over per-round blocks, with one optimiser step per block. The decoder used 10 unrolled layers, each with a 1D CNN denoiser (32 filters, kernel size 3). The Bayesian-CNN mixing weight was initialised at 0.85. MSE loss was unit-weighted, with $\lambda_1 = 0.01$, $\lambda_W = 0.001$, and $\lambda_K = 0.01$.

4. RESULTS & ANALYSIS

The proposed method was compared with the AMP-DA baseline². The datasets were split 20% IID and 80% non-IID, with 10,000 samples randomly assigned across devices and the remaining 40,000 label-sorted into contiguous shards, distributed sequentially to each device. The number of active devices K_a was drawn uniformly from [7, 13]. The global model was updated using FedAvg, with update fragment size of 20, and URA codeword length of 64. Fig. 3 and Table 1 show that the proposed method consistently outperforms AMP-DA, improving reliability in higher SNR regimes while providing significantly stronger recovery and more stable convergence in lower SNRs. The reliability of active device estimation (Fig. 4) was also greatly improved, with final estimates consistently within ± 0.5 tolerance required. This is critical for scaling the global up-

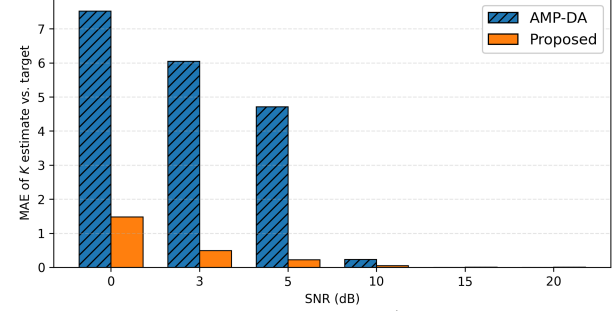


Fig. 4. Mean average error for \hat{K}_a (unrounded).

date correctly (Eq (4)) since underestimation causes instability while overestimation slows convergence.

Table 1. Final test accuracies across SNR levels (dB).

Method \ SNR	0	3	5	10	15	20
AMP-DA	0.139	0.135	0.525	0.801	0.799	0.805
Proposed	0.690	0.788	0.794	0.804	0.803	0.805

Note: PA accuracy reference (no channel): 0.804.

To directly test generalisation, dataset collection and pre-training were ran using a ResNet global model, while inference trained a simpler CNN at 5 dB SNR [12]. Results showed that there was no noticeable reduction in convergence performance, demonstrating the proposed method generalised effectively. This is largely by design, as quantisation and sparse coding reduce the task to recovering integer indices, while codebook ordering makes codeword usage more predictable. Together, these choices simplify decoding so that unseen setups resemble those encountered during training.

The effects of codebook initialisation, learning and ordering are shown in Table 2 demonstrating the benefits of learning the URA codebook and applying popularity ordering. Subsequent analysis of the URA codebook showed that it learnt to reduce pairwise cross-correlation more for popular codewords, while tolerating higher correlation for unpopular ones. Singular value analysis, measuring the spread of SVD decomposition's diagonal entries, also showed a reduced range indicating better conditioning than fixed baselines.

Table 2. Codebook setup evaluation accuracy, SNR = 5 dB.

Codebook	Initialisation	Ordering	Accuracy
Learnt	Data-driven	Popularity	0.949
Learnt	Gaussian	Popularity	0.932
Learnt	Data-driven	None	0.877
Fixed	Data-driven	None	0.666
Fixed	Gaussian	None	0.696
Fixed	Bernoulli	None	0.689

5. CONCLUSIONS

This paper presented a digital OTA FEEL solution, combining a learnt decoder (AMP-DA-Net) with a jointly trained URA codebook. The method retains the same uplink cost as the state-of-the-art, while extending reliable operation by more than 7 dB. Results show strong improvements in recovery and stability, particularly under challenging low-SNR conditions, and analysis confirms the approach generalises well to unseen setups, different participation levels and highly non-IID devices. Future work will explore an extended setup of multi-antenna fading channel.

²All code available at <https://github.com/tonytarizzo/AMP-DA-Net>

6. REFERENCES

- [1] Brendan McMahan, Eider Moore, Daniel Ramage, Seth Hampson, and Blaise Aguera y Arcas, “Communication-efficient learning of deep networks from decentralized data,” in *Int'l Conf. on Artificial Intelligence and Statistics (AISTATS)*. Apr 2017, vol. 54, pp. 1273–1282, PMLR.
- [2] Jakub Konečný, H. Brendan McMahan, Felix X. Yu, Peter Richtárik, Ananda Theertha Suresh, and Dave Bacon, “Federated learning: Strategies for improving communication efficiency,” Oct 2016.
- [3] Ninghui Jia, Zhihao Qu, Baoliu Ye, Yanyan Wang, Shihong Hu, and Song Guo, “A comprehensive survey on communication-efficient federated learning in mobile edge environments,” *IEEE Comm. Surveys & Tutorials*, 2025.
- [4] Mingzhe Chen, Deniz Gündüz, Kaibin Huang, Walid Saad, Mehdi Bennis, Aneta Vulgarakis Feljan, and H. Vincent Poor, “Distributed learning in wireless networks: Recent progress and future challenges,” *IEEE Journal on Selected Areas in Communications*, vol. 39, no. 12, pp. 3579–3605, 2021.
- [5] Alham Fikri Aji and Kenneth Heafield, “Sparse communication for distributed gradient descent,” in *Conf. on Empirical Methods in Natural Language Proc. (EMNLP)*, Copenhagen, Denmark, Sep 2017.
- [6] Emre Ozfatura, Kerem Ozfatura, and Deniz Gündüz, “Time-correlated sparsification for communication-efficient federated learning,” in *2021 IEEE International Symposium on Information Theory (ISIT)*, 2021, pp. 461–466.
- [7] Dan Alistarh, Demjan Grubic, Jerry Li, Ryota Tomioka, and Milan Vojnovic, “QSGD: Communication-efficient SGD via gradient quantization and encoding,” 2017.
- [8] Jeremy Bernstein, Yu-Xiang Wang, Kamyar Azizzadenesheli, and Anima Anandkumar, “signSGD: Compressed optimisation for non-convex problems,” in *Int'l Conference on Machine Learning (ICML)*. Jul 2018, vol. 80, pp. 560–569, PMLR.
- [9] Frank Seide, Hao Fu, Jasha Droppo, Gang Li, and Dong Yu, “1-bit stochastic gradient descent and its application to data-parallel distributed training of speech DNNs,” in *InterSpeech 2014*, Sep 2014, pp. 1058–1062.
- [10] Mohammad Mohammadi Amiri and Deniz Gündüz, “Machine learning at the wireless edge: Distributed stochastic gradient descent over-the-air,” *IEEE Trans. on Signal Proc.*, vol. 68, pp. 2155–2169, 2020.
- [11] Mohammad Mohammadi Amiri and Deniz Gündüz, “Federated learning over wireless fading channels,” *IEEE Trans.s on Wireless Comms.*, vol. 19, no. 5, pp. 3546–3557, 2020.
- [12] Yuxuan Sun, Sheng Zhou, Zhisheng Niu, and Deniz Gündüz, “Dynamic scheduling for over-the-air federated edge learning with energy constraints,” *IEEE Journal on Selected Areas in Communications*, vol. 40, no. 1, pp. 227–242, Jan 2022.
- [13] Guangxu Zhu, Yuqing Du, Deniz Gündüz, and Kaibin Huang, “One-bit over-the-air aggregation for communication-efficient federated edge learning: Design and convergence analysis,” *IEEE Trans. on Wireless Comms.*, vol. 20, no. 3, Mar 2021.
- [14] Li Qiao, Zhen Gao, Mahdi Boloursaz Mashhadi, and Deniz Gündüz, “Massive digital over-the-air computation for communication-efficient federated edge learning,” *IEEE Journal on Selected Areas in Communications*, vol. 42, no. 11, pp. 3078–3094, Nov 2024.
- [15] Shuyan Hu, Xin Yuan, Wei Ni, Xin Wang, Ekram Hossain, and H. Vincent Poor, “Ofdma-f²l: Federated learning with flexible aggregation over an ofdma air interface,” *IEEE Trans. on Wireless Comms.*, vol. 23, no. 7, Jul 2024.
- [16] Alphan Şahin, Bryson Everette, and Safi, “Distributed learning over a wireless network with fsk-based majority vote,” *arXiv preprint arXiv:2111.01850*, Nov 2021.
- [17] Yury Polyanskiy, “A perspective on massive random-access,” in *2017 IEEE International Symposium on Information Theory (ISIT)*, Jun 2017, pp. 2523–2527.
- [18] Sihua Wang, Mingzhe Chen, Cong Shen, Changchuan Yin, and Christopher G. Brinton, “Digital over-the-air federated learning in multi-antenna systems,” *IEEE Transactions on Wireless Communications*, vol. 23, no. 6, pp. 4184–4198, Jun 2024.
- [19] Tian Li, Anit Kumar Sahu, Manzil Zaheer, Maziar Sanjabi, Ameet Talwalkar, and Virginia Smith, “Federated optimization in heterogeneous networks,” in *Conf. on Machine Learning and Sys. (MLSys)*, Apr 2020, vol. 2.
- [20] Alphan Sahin, “On the feasibility of distributed phase synchronization for coherent signal superposition,” in *IEEE PIMRC Workshops - Integrated, Intelligent and Ubiquitous Connectivity for 6G and Beyond*, Sep 2025.
- [21] David Arthur and Sergei Vassilvitskii, “k-means++: The advantages of careful seeding,” in *Annual ACM-SIAM Symp. on Discrete Algs. (SODA'07)*, New Orleans, LA, Jan 2007.
- [22] Sundeep Rangan, “Generalized approximate message passing for estimation with random linear mixing,” in *IEEE Int'l Symp. on Inform. Theory (ISIT)*, Jul 2011.
- [23] Zhonghao Zhang, Yipeng Liu, Jianli Liu, Fei Wen, and Ce Zhu, “Amp-net: Denoising-based deep unfolding for compressive image sensing,” *IEEE Transactions on Image Processing*, vol. 30, pp. 1487–1500, Mar 2021.
- [24] Kartheek K. R. Nareddy, Inbasekaran Perumal, and Chandra Seelamantula, “Some intriguing observations on the learnt matrices in deep unfolded networks,” in *IEEE Intl Conf. on Acoustics, Speech and Signal Proc. (ICASSP)*, Apr 2025.
- [25] Kaiming He, Xiangyu Zhang, Shaoqing Ren, and Jian Sun, “Deep residual learning for image recognition,” *2016 IEEE Conference on Computer Vision and Pattern Recognition (CVPR)*, p. 770–778, Jun 2016.
- [26] Yongxin Zhu, Bocheng Li, Yifei Xin, and Linli Xu, “Addressing representation collapse in vector quantized models with one linear layer,” 2024.
- [27] Jian Zhang and Bernard Ghanem, “Ista-net: Interpretable optimization-inspired deep network for image compressive sensing,” in *IEEE/CVF Conf. on Comp. Vision and Pattern Recog. (CVPR)*, 2018.